The Astrophysical Journal Letters, 910:L8 (9pp), 2021 March 20 https://doi.org/10.3847/2041-8213/abebe6

Climate Change of over 20 °C Induced by Continental Movement on a Synchronously Rotating Exoplanet

Zhouqiao Zhao, Yonggang Liu, Weihan Li, Haobo Liu, and Kai Man
Department of Atmospheric and Oceanic Sciences, School of Physics, Peking University, Beijing, 100871, People's Republic of China; ygliu@pku.edu.cn
Received 2020 December 12; revised 2021 February 12; accepted 2021 February 26; published 2021 March 23

Abstract

It is generally believed that the addition of continents cools the climate of an aquaplanet with a similar orbit to Earth; this is because continents have a higher surface albedo than oceans. A similar effect has been shown in climate simulations for exoplanets. Here we demonstrate that the influence of a continent on ocean circulation could have a dominative effect on the climate of a synchronously rotating exoplanet compared with the effect of the surface albedo, especially when the rotation of the exoplanet is relatively slow (e.g., the rotational period is 40 Earth days). The global mean surface temperature could vary by more than 26° C, simply by moving a small continent to a different location. The ocean circulation on a synchronously rotating exoplanet is characterized by a strong westerly jet along the equator and one large gyre in each hemisphere. The surface temperature decreases when the equatorial westerly or the western branch of either of the gyres is blocked by a continent or an island arc chain. However, if the continent blocks the eastern branch of the gyre, the equatorial westerly is strengthened and the climate warms. A large number of potentially habitable exoplanets have been found orbiting around M-dwarfs in a tidally locked manner; our results indicate that their climates, as well as their atmospheric chemistry, may deviate from previous estimates if a small continent, or even an island arc chain, is present.

Unified Astronomy Thesaurus concepts: Exoplanet dynamics (490); Exoplanets (498); Extrasolar rocky planets (511); Habitable planets (695); Exoplanet atmospheres (487); Planetary climates (2184); Ocean planets (1151)

1. Introduction

The recent discovery of abundant exoplanets (Dressing & Charbonneau 2015; Morley et al. 2017), especially those nearby and potentially habitable such as Proxima Centauri b (Anglada-Escude et al. 2016), TRAPPIST-1e (Gillon et al. 2017), and LHS 1140b (Dittmann et al. 2017), has greatly expanded our understanding of the universe. The habitable zone (HZ) herein is defined as the region around a star in which liquid water can be maintained on the surface of a terrestrial planet (Kasting et al. 1993). It is estimated that approximately 75% of the stars in galaxy are M-dwarfs, and one-sixth of M-dwarfs have at least one Earth-sized planet orbiting in their HZ (Dressing & Charbonneau 2015). These exoplanets are ideal searching targets for real habitable exoplanets and alien life.

The HZ around M-dwarfs falls almost entirely in the tidally locked zone (Kasting et al. 1993), in which the rotational period and orbital period of planets are equal (Barnes 2017). Such planets are also described as synchronously rotating. The climate of a synchronously rotating exoplanet depends on its orbital period, and can be warmed by approximately 40° C when the orbital period is accelerated from 256 Earth days to 1 Earth day (Yang et al. 2014). This is because the Rossby deformation radius of the atmosphere is smaller when the orbital period is shorter. A smaller deformation radius will cause the cloud belt around the equator to be narrower and thus reflects less stellar insolation (Edson et al. 2011; Yang et al. 2014; Noda et al. 2017; Haqq-Misra et al. 2018).

Adding a continent under the substellar point cools the exoplanet. The global mean annual surface temperature (GMST) decreases only slightly when the size of the continent at the substellar point is small (e.g., ∼5% of the planetary surface area), but can decrease by 10° C as the size of the continent is increased to 40% of the planetary surface area (Lewis et al. 2018; Salazar et al. 2020). However, to the best of our knowledge, to date there is no systematic study of the influence of continental location on the climate of a synchronously rotating exoplanet. The cooling effect of terrestrial land on the Earth is mildly dependent on the latitudinal locations of continents, and can induce a difference in the GMST by a few degrees Celsius (Poulsen 2002; Liu et al. 2013). In contrast, the GMST can change by more than 20° C on a synchronously rotating exoplanet when a small continent is moved, as will be described.

In Section 2, the model setting and experimental design are described. The results are then described in Section 3 and mechanisms are discussed in Section 4.

2. Method

The climate of an Earth-sized terrestrial planet synchronously rotating around an M-dwarf is studied using an atmosphere-ocean general circulation model (AOGCM), Community Climate System Model version 3 (CCSM3; see Appendix A.1 for more details). The model includes dynamic sea-ice and land-surface processes, e.g., soil moisture and river runoff. The surface temperature of the M-dwarf is assumed to be 4000 K. The redshift of the stellar spectrum compared with the Sun is considered. This shift reduces the ice and snow albedo (Yang et al. 2019). The solar constant is set to 1000 W m^{-2}, and the CO_2 volume mixing ratio (co2vmr) is set to 10%. The solar constant and greenhouse condition are set such that liquid water can be maintained on the aquaplanet surface in both slow- and fast-rotating schemes. An idealized round continent with a radius of 20° (3% of the planet surface area; Figure 1) is placed at 50 different locations between 90° East (E) ∼ 90° West (W) and 0° ∼ 80° North (N) over the dayside (see Figure A1 in the Appendix). The substellar point is at (0° N, 0° E). Cases with a continent located in the southern

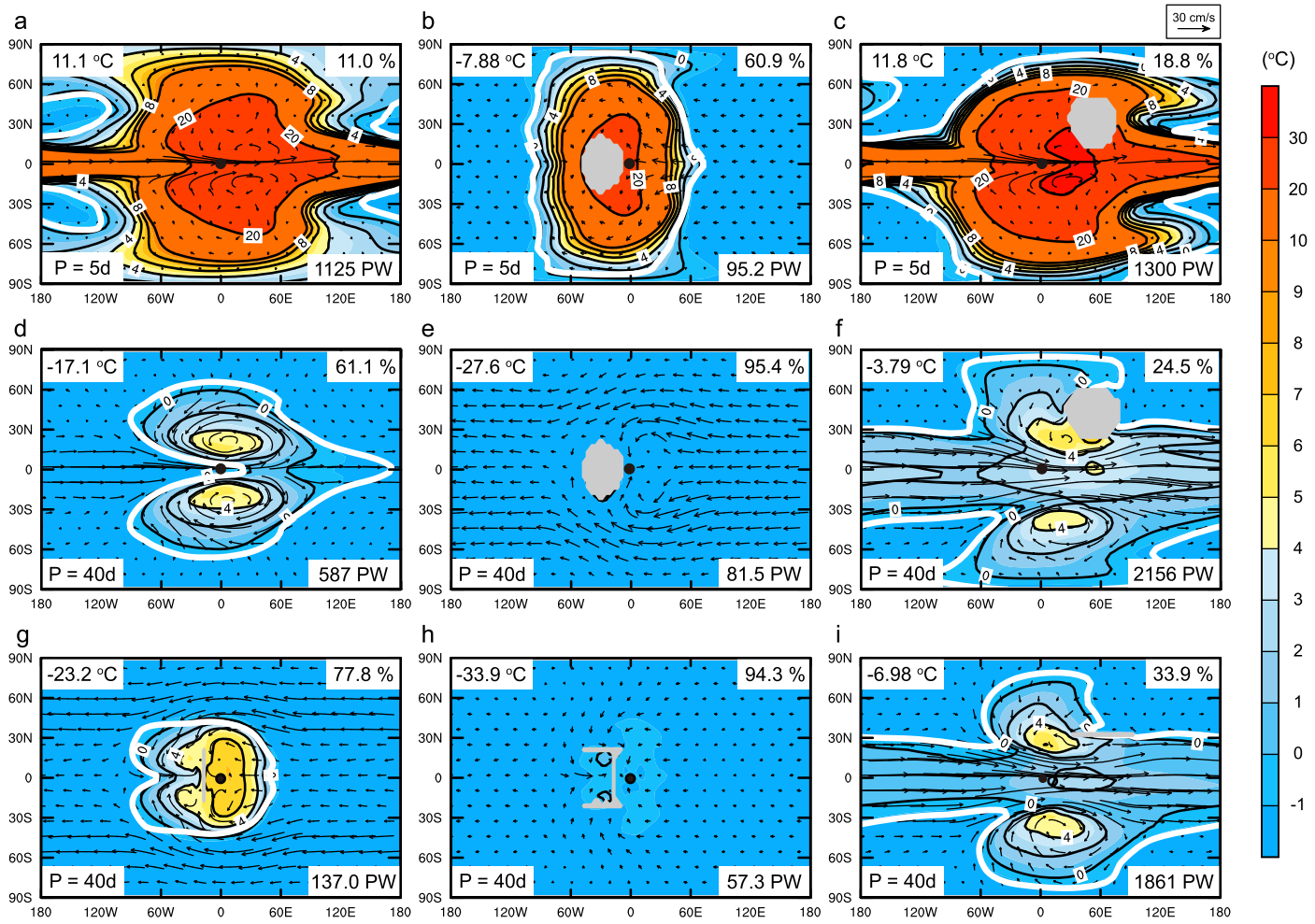

Figure 1. Sea-surface temperature and current and ice edges for selected cases. The GMST, global sea-ice fraction, and ocean heat transport from dayside to nightside are marked in the top-left, top-right, and bottom-right corners, respectively. Ice edges are indicated by thick white curves. The rotational period is 5 days in (a)–(c) and 40 days in (d)–(i). (a) and (d) are an aquaplanet. The center of the round continent is at (0° N, 30° W) in (b), (e), (30° E, 50° N) in (c), and (40° E, 50° N) in (f). The bar-shaped continent in (g) is located at 20° W and extends from 20° South (S) to 20° N. The bar-shaped continent in (i) is located at 20° N and extends from 30° E to 90° E. Because of the low resolution and non-uniform meridional resolution of the ocean module, the shape of the continent is distorted from a perfect circle.

hemisphere are not tested because their climates would be identical to those with continent located in the northern hemisphere when flipped around the equator. Tests are done for both fast-rotating (rotational period $P = 5$ days) and slow-rotating ($P = 40$ days) exoplanets.

To differentiate the albedo effect and oceanic dynamic effect of the continent on climate, two sets of sensitivity experiments are carried out. In the first set, a virtual continent is placed at various locations in an aquaplanet. The virtual continent has the same shape as that of a real continent, but a manually set high albedo affects the surface radiation only (orange region in Figures 3 and 4). The downward shortwave radiation is reduced by 90% over ocean and ice whenever a virtual continent is encountered. The virtual land could mimic a high-albedo region that does not affect ocean circulation. In the second set, the continent is represented by a narrow bar (gray bars in Figure 1) so as to minimize its albedo effect. This bar-shaped continent may be representative of an island arc chain.

3. Results

Climates are different for exoplanets in the slow-rotating and fast-rotating regimes (Edson et al. 2011; Yang et al. 2014; Noda et al. 2017; Haqq-Misra et al. 2018), and so are their responses to continental location. For an aquaplanet, the GMST is much higher in the fast-rotating cases compared with the slow-rotating ones (11.1° C versus −17.1° C; compare Figures 1(a) and (d)). When a continent is present, the minimum GMSTs are −7.9° C and −27.6° C for $P = 5$ days and 40 days, respectively, both obtained when the continent is located at ∼30° W on the equator (Figures 1(b), (e), 2(a) and (d)). The warmest climate is obtained when the continent is located to the northeast of the substellar point. For $P = 5$ days, the maximum GMST is 11.8° C (Figure 1(c)), only slightly higher than that of an aquaplanet. However, the maximum GMST for $P = 40$ days is −3.8° C (Figure 1(f)), 13.3° C higher than that of an aquaplanet (−17.1° C; Figure 1(d)). This warmest climate is obtained when the continent is located at (40° N, 50° E). In any case, the GMST varies by ∼20° C or more by simply changing the location of a small continent. Note that the coldest climate in the $P = 40$ days case (Figure 1(e)) is a snowball state, in which sea ice covers the ocean completely.

The virtual continent induces a cooling effect on the climate. Although the albedo of the virtual continent has been greatly exaggerated (surface albedo for virtual land is set to 90%, compared with the typical value for terrestrial land around

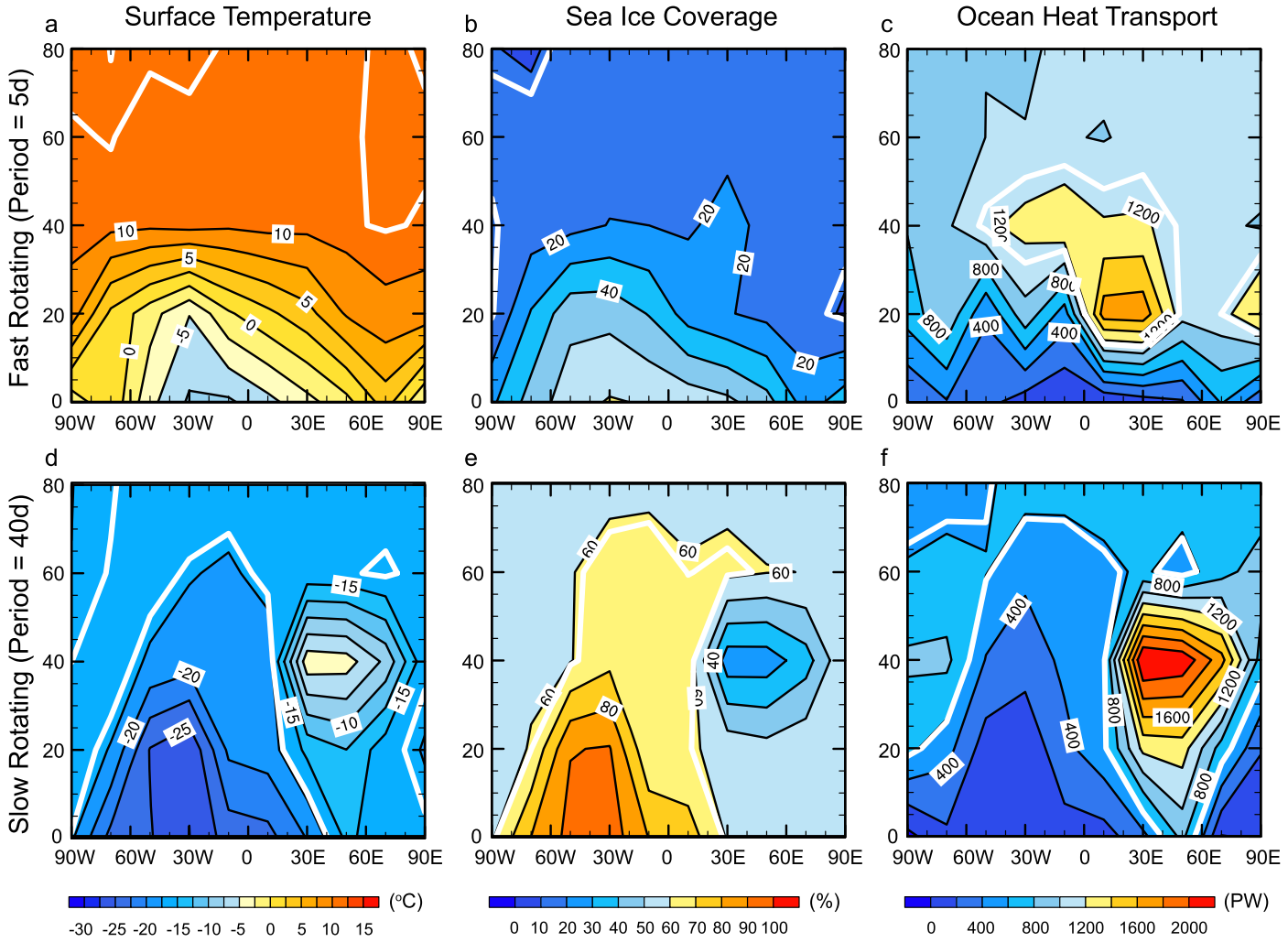

Figure 2. Summary of GMST (a), (d), global sea-ice fraction (b), (e), and dayside-to-nightside ocean heat transport (c), (f) for all cases with round continent. The rotational period is 5 days and 40 days in (a)–(c) and (d)–(f), respectively The corresponding value for an aquaplanet is marked with the white contour line.

20%–30%), it does not induce much cooling for the $P = 40$ days case, certainly not enough to produce a snowball state (Figures 3(c), (f), 4(a)–(b) and (d)–(e)). In greater contrast to the real continent, a virtual continent cannot warm the climate, no matter where it is located. For the $P = 5$ days case, the cooling effect of the virtual continent is more significant, especially when it is located on the equator (Figures 4(a)–(b)).

For both the fast- and slow-rotating exoplanets, a meridionally oriented stick-style continent cools the planet when located on the equator. The GMST is decreased by 11° C and 6° C in fast- and slow-rotating schemes, respectively, when the continent is located at 20° W (Figures 1(g) and 4(c)). A zonally oriented stick-style continent, when located to the northeast of the substellar point, can raise the GMST by up to 10° C for the slow-rotating exoplanet, similar to the effect of a round terrestrial land.

4. Discussion

4.1. Albedo Effect

The sensitivity of a climate to the location of the virtual continent (Figures 3(c), (f), 4(a)–(b), and (d)–(e)) is governed by the spatial pattern of sea ice and cloud (Figure 3). The downwelling shortwave radiation at the surface is generally higher for the fast-rotating exoplanet than for the slow-rotating one (compare Figures 3(b) and (e)) due to the weaker shortwave cloud forcing in the former (Figures 3(a) and (d); Yang et al. 2013, 2014). Moreover, the downwelling shortwave radiation at the surface in the fast-rotating exoplanet is highly non-uniform with a peak near the substellar point, and decreases away from this point (Figure 3(b)). As a result, the high-albedo virtual continent placed near the substellar point could cool the fast-rotating planet much more efficiently than when it is placed elsewhere.

For the slow-rotating exoplanet, the heaviest clouds occur to the east of the substellar point off the equator and lighten gradually away from these two points (blue regions in Figure 3(d)). Such cloud distribution makes the downward stellar radiation received at the surface quite uniform over the dayside, except a small region to the west of the substellar point (Figure 3(e)). In this small region, however, sea ice is prevalent (Figure 1(d)); adding a virtual continent here does not reflect more stellar insolation than elsewhere. Therefore, a virtual continent has a relatively stronger cooling effect when located in the mid-latitudes (Figures 4(e)), where both the cloud amount and sea-ice concentration are low, than when located near the substellar point (Figure 4(d)).

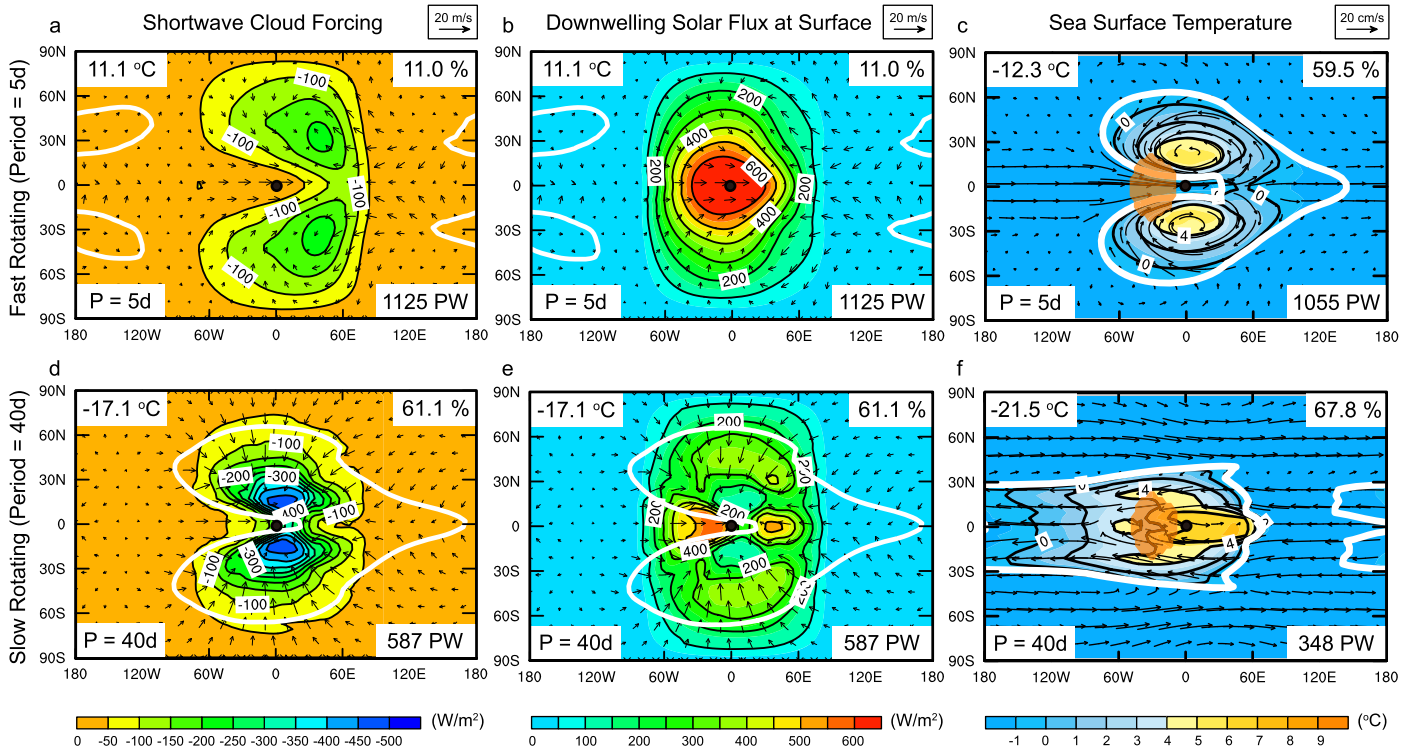

Figure 3. Shortwave cloud forcing (a), (d) downwelling solar radiation received at the surface (b), (e) and sea-surface temperature (c), (f) in aquaplanets. The rotational period is 5 days and 40 days in (a)–(c) and (d)–(f), respectively. The arrows show surface wind (a), (b), (d), and (e) and ocean current (c), (f). (c), (f) sea-surface temperature in the case with round high-albedo virtual land. Ice edges are indicated by thick white curves. In (c) and (f), a virtual continent (orange) is placed at (30° W, 0° N) which reflects sunlight but does not block ocean currents.

4.2. Ocean Circulation and Ocean Heat Transport

The ocean circulation on a synchronously rotating exoplanet is characterized by a strong equatorial westerly and two cyclonic gyres on either side of the equator (Figures 1(a) and (d)). Such a pattern is very similar to the Matsuno–Gill mode that has been well studied for the atmosphere (Matsuno 1966; Gill 1980; Showman & Polvani 2010, 2011), and has been obtained for exoplanets in many previous studies (Hu & Yang 2014; Del Genio et al. 2019; Yang et al. 2019). As P decreases from 40 days to 5 days, the size of the gyres shrinks (compare Figure 1(a) to Figure 1(d)) due to reduction of the Rossby deformation radius of the ocean (see Figure A2 in the Appendix). Unlike the strong western boundary ocean current on Earth, which can occur on any longitude along a coast and thus is difficult to block, the westerly jet on the synchronously rotating exoplanet is restrained to the equator. Such a current is susceptible to blocking by a continent.

The equatorial westerly could explain more than 87% of oceanic heat transport from dayside to nightside (see Figure A3 in the Appendix), due to the substantial ocean current speed and temperature difference between the dawn terminator (90° W) and night terminator (90° E) (Figures 1(a) and 1d). Moreover, both the global surface temperature (see Figure A3(a) in the Appendix) and global sea-ice fraction (see Figure A3(c) in the Appendix) have a good linear relationship with the total dayside-to-nightside ocean heat transport (Figure 2). When the equatorial westerly is blocked by a round continent or a meridionally oriented bar-shaped continent (Figures 1(b), (e), (g)–(h) and 4(c)), the sea ice drifts from the nightside to dayside under wind forcing (Figures 1(b) and (e)). This sea-ice transport induces cooling of the dayside. This is why the continent induces the coldest climate when located at (0° N, 30° W).

The eastward momentum is imported into and taken out of the equatorial westerly by the western and eastern branches of the ocean gyres, respectively (Figures 1(g)–(i) and 4(c)). A near-complete blocking of the westerly can be achieved by a meridionally oriented bar-shaped continent (Figure 1(g)). Further weakening of the westerly can be achieved by blocking the western branches of the gyres by adding two zonal bars (Figure 1(h)). When the round continent lies at (0° N, 70° W), the momentum import is partially blocked and the equatorial westerly remains strong. In this case, the GMST is similar to that in an aquaplanet, although the equatorial westerly is not as strong; the nightside is cooler but the dayside is warmer because sea-ice import into the dayside from the dawn terminator is blocked by the continent. When the continent is moved to the east of substellar point, the equatorial westerly hits the continent and is diverted toward the high latitude (Figure 4(f)). The energy carried by the diverted ocean currents warms the high latitudes and increases the GMST.

On the other hand, if the eastern branch of the gyre circulation is blocked by a continent so that the momentum export is sequestered, a strengthening of the equatorial westerly happens. The strengthening of this westerly will warm up the planet by transporting more heat from the dayside to the nightside. This is clearly seen by comparing Figures 1(f) and (i) to Figure 1(d). Note that for the fast-rotating exoplanet, its climate becomes insensitive to dayside-to-nightside ocean heat transport once the transport is larger than approximately 500 petawatts (PW; green symbols in Figure A3(a) and (c) in the Appendix). This insensitivity is probably because the climate is already very warm in the aquaplanet configuration, to such a

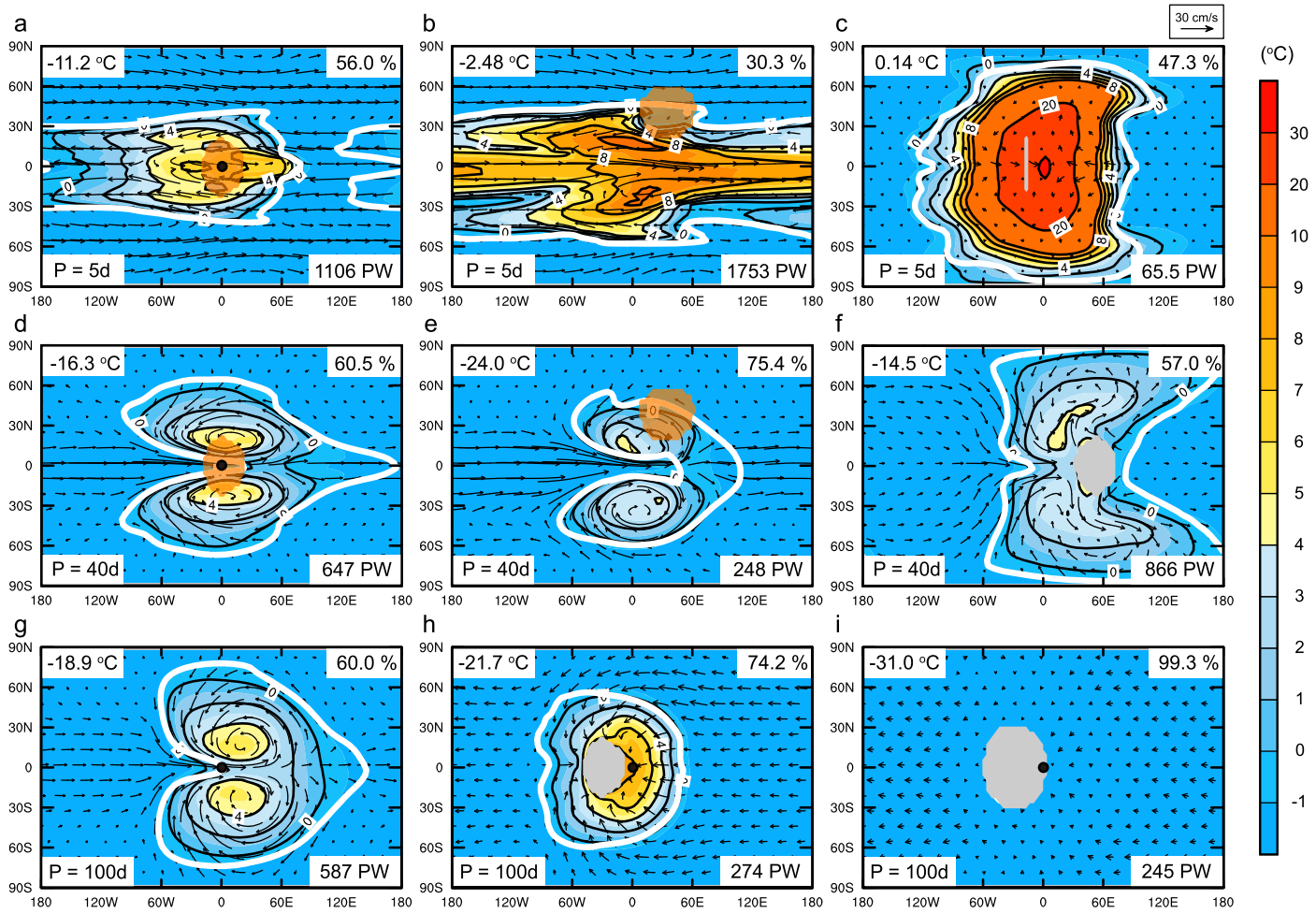

Figure 4. Sea-surface temperature and current and ice edges for selected cases. The GMST, ice fraction, and ocean heat transport from dayside to nightside are marked in the top-left, top-right, and bottom-right corners, respectively. Ice edges are indicated by thick white curves. The rotational period is 5 days in (a)–(c) and 40 days in (d)–(i). (a) and (d) are aquaplanets. The virtual continent (orange) is placed at (0° N, 0° W) in (a), (d), (40° N, 30° E) in (b), (f), and (40° N, 30° W) in (e). The round continent (gray) is located at (0° N, 90° W), (0° N, 50° E), and (0° N, 90° E) in (g)–(i), respectively.

degree that there is no sea ice in the dayside and little sea ice in the nightside (Figure 1(a)); further energy transport to the nightside does not induce a reduction of sea ice cover in the dayside. Therefore, the warming effect when blocking the eastern branch of gyre circulations in a fast-rotating exoplanet is negligible (compare Figures 1(c) to (a)), at least for the base climate tested here.

4.3. Effect of Continental Size and Shape

When the radius of continent is reduced by half to 10°, its climate impact weakens. The GMST is 1.04° C and −21.5° C (not shown) for $P = 5$ days and 40 days, respectively, when this small continent is placed at (0° N, 30° W), as compared to −7.9° C and −27.6° C when the continental radius is 20° (Figure 1). The continent has to be large enough to fully block the relevant ocean currents in order to influence the climate effectively. Because the spatial scale of ocean currents is dependent on the rotational period, the minimum size of the continent required is also dependent on the rotational period. For example, when the rotational period is increased to 100 days, the spatial scale of ocean gyres is enlarged (Figure 4(g)). As a result, the radius of continent needs to be increased to ∼30° in order to produce a snowball state when the continent is placed at (0° N, 30° W) (Figures 4(h)–(i)). As long as the continent can block the relevant ocean currents, the shape of the continent is not important. It has been demonstrated in Figure 1 that a combination of simple linear continental structures can perform as well as a two-dimensional continent.

4.4. Implication for Planetary Habitability and Atmospheric Chemistry

Since the continental location affects climate considerably, it should have an impact on the width of the HZ. Here we test only the shift of the outer edge of HZ due to presence of a continent. It is found that when a continent is located to the northeast of the substellar point, global glaciation will not occur until solar constant is reduced below 840 W m^{-2}. However, when a continent lies to the west of the substellar point on equator, the planet would be almost completely frozen when the solar constant is 1000 W m^{-2}. As a result, the outer edge could differ by ∼160 W m^{-2} if a small continent is present and its location varies (Figure 5). Our results thus suggest that the climate and habitability of a synchronously rotating exoplanet is highly dependent on the details of continental distribution.

The nutrient supply at the ocean surface is essential for the flourishing of life. Previous studies have shown that the ocean mixing layer could be deepened and the upwelling could be

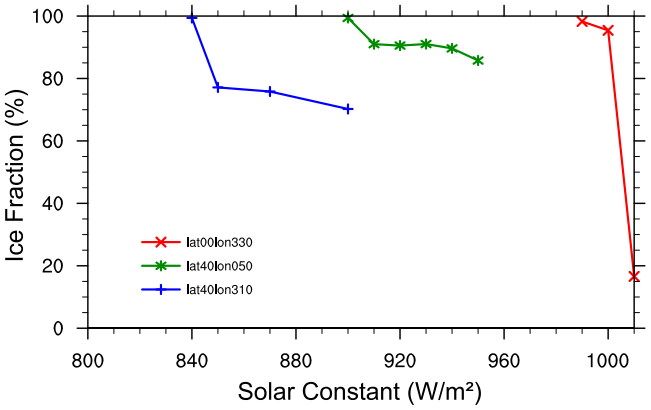

Figure 5. Outer edge of the HZ for different locations of a round continent. The edges are calculated only when the continent is located at (30° W, 0° N) (red line), (50° E, 40° N) (green line), and (50° W, 40° N) (blue line). The edges are assumed to be reached when the global sea-ice fraction reaches 100%.

strengthened as the rotation slows down (Olson et al. 2020). For aquaplanets, the global mean mixed-layer depth and the total upwelling at the base of the mixed layer over ice-free dayside are approximately 86 m and 127 Sv, respectively, when $P = 5$ days. These values increase to 135 m and 214 Sv, respectively, when P is increased to 40 days. When there is a continent, the upwelling may be enhanced along certain parts of the coastline. However, the changes in total upwelling with the change in continental location are dominated by the changes in upwelling over the open ocean; both the area of the open ocean and the intensity of upwelling change when the continental location changes (see Figure A4 in the Appendix). The total upwelling over ice-free dayside can be as small as 50 Sv when the continent lies on the equator, but can increase to ∼250 Sv in the fast-rotating scheme and ∼1000 Sv in the slow-rotating scheme when it lies to the northeast of the substellar point (see Figure A4 in the Appendix). Such a strong upwelling over the dayside not only enhances the biological activity, but also may amplify the contrast in biosignatures between the dayside and nightside (Chen et al. 2018). Both the large absolute abundance and the large contrast between the dayside and nightside of these biosignatures facilitate remote detection.

The presence of a continent may affect the abundance and the spatial distribution of ozone too, since the availability of water vapor is critical for the destruction of ozone (Peyrous 1990). In previous studies of ozone distribution on synchronously rotating exoplanets, the ocean was represented as a mixed layer with no horizontal movement and the influence of continents was either not considered or underestimated (Chen et al. 2018, 2020; Yates et al. 2020). When both ocean circulation and continent are considered simultaneously, as has been done here, the temperature over the nightside changes with the location of the continent, and the specific humidity in the atmosphere changes accordingly. The atmospheric mass transport above 200 hPa from the dayside to nightside also changes with the location of the continent, especially for the fast-rotating case; for $P = 5$ days, this transport can increase from 7 gigatons per second (Gt s^{-1}) in an aquaplanet to 14 Gt s^{-1} when the continent is located to both the northeast and northwest of the substellar point (not shown). This transport brings along with it the ozone and water vapor; it is unclear how the change of this transport will affect the ozone of the dayside. Therefore, AOGCMs are required to fully understand the ozone distribution on these exoplanets when a continent is present.

5. Conclusion

We investigate the climate impact of a relatively small terrestrial continent on a synchronously rotating exoplanet by using an AOGCM. It is found that the climate is highly sensitive to the location of the continent, mainly because of the existence of a strong equatorial westerly jet in the ocean on such exoplanets. This jet is responsible for ∼90% of the heat transport from dayside to nightside, and the strength of this jet largely determines the global climate. When a continent blocks the equatorial westerly at the equator, the climate cools. The strongest cooling effect is obtained when it lies slightly to the west of the substellar point. On the other hand, the westerly jet strengthens and the climate warms when a continent obstructs the poleward branch of the oceanic gyre circulation. Enhanced oceanic heat transport to the nightside reduces the sea ice coverage there, and thereby reduces the sea-ice input from nightside to dayside. This reduces the planetary albedo and raises the GMST. The GMST can vary by more than 20° C simply by varying the location of a small continent. The outer edge of the HZ around an M-dwarf defined by stellar constant can change by 15% when a small continent is located at different places. Because the atmospheric circulation, atmospheric water vapor, and ocean upwelling all change with the location of the continent, the atmospheric chemistry and biosignatures may also change.

Although major topographic features tend to align with the star-planet axis for synchronously rotating exoplanets (Wieczorek 2007; Turbet et al. 2016; Salazar et al. 2020), small continents or island arc chains may exist everywhere. Our results demonstrate that these small features can still change the global climate of a synchronously rotating exoplanet by as much as that of a round continent. We also demonstrate that it is possible to engineer the climate on such exoplanets by building a dam at appropriate locations.

We are grateful to J. Yang for discussion and Y. Si for the help on modifying the source code. We acknowledge support from the National Natural Science Foundation of China (NSFC) grants 41875090 and 41761144072. The computation was supported by the High-performance Computing Platform of Peking University.

Appendix
Model and Experimental Design

A.1. Climate Model

The simulations presented in this work were done with the fully coupled AOGCM CCSM3 (Collins et al. 2006). The model is the same as that used by Yang et al. (2019). The atmosphere and land share the same Gaussian grid, and the ocean and sea ice share the same grid. The resolution of the CCSM3 model is set to "T31_gx3v5." In this setting, the horizontal grid spacing is approximately 3.75° by 3.75° for the atmosphere and land. The grid spacing for the ocean and sea ice is 3.6° in the zonal direction but highly non-uniform in the meridional direction, with its value as small as 0.6° near the equator and as large as ∼3° around mid-latitude. The atmosphere and ocean have 26 and 25 vertical layers, respectively.

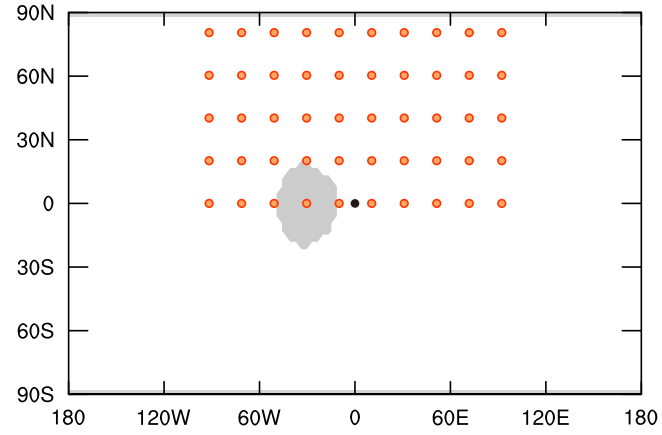

Figure A1. Locations (orange) of the center of the round continent in 50 experiments carried out for each rotational period. One example of the continent (gray) is given. The black dot marks the substellar point.

All the experiments were run for at least 400 Earth years. Experiments with near-snowball state were continued for 600 Earth years in order to achieve statistical equilibrium. Normally, the last 50 yr of simulations were averaged for analyses. However, some experiments have strong multi-decadal climate oscillations after reaching statistical equilibrium. For these experiments, the last 150 yr of data are used for analyses.

A.2. Planetary Properties

The exoplanet herein is assumed to have similar physical properties, e.g., radius and gravity, to those of the Earth. The orbital and rotational periods of the planet are equal and can be either 5 or 40 Earth days (d). The obliquity, eccentricity, and precession are all set to 0. Previous studies have demonstrated that the climate impact of planetary gravity on synchronously rotating exoplanet is small, and the ice fraction changes by less than 10% when gravity increases from 5 to 35 m s^{-2} (Yang & Abbot 2014; Yang et al. 2019).

A round, flat continent with a radius of 20° is placed at different locations in different experiments (Figure A1). The bar-shaped continent has a width of ∼5°. Two small, round islands with a radius of ∼5° are added in the south and north poles to avoid the singularity there in the ocean model. The ocean depth is set to 1500 m. All experiments are initiated with an ice-free state; the ocean has a uniform temperature of 0° C and salinity of 35 psu.

The stellar constant is set to be 1000 W m^{-2} in most cases. The stellar spectra are set to be the emission spectra of a 4000 K blackbody. The redshift of stellar spectra relative to that of Sun reduces ice albedo since ice albedo in the infrared band is lower than that for the visible band (Shields et al. 2014). Only when the outer edge of the HZ is searched is the stellar constant varied. The atmospheric composition and pressure are assumed to be similar to that of Earth as well. The partial pressure of CO_2 is set to 0.1 bar in all experiments.

The Rossby deformation radius stands for the spatial scale of geostrophic balance (between the horizontal pressure gradient and the Coriolis force), or the spatial scale of the region that is influence by a disturbance in the geostrophic adjustment. On Earth, the Rossby deformation radius in the ocean is small (∼200 km in low latitudes, which decreases to ∼10 km in polar regions; Chelton et al. 1998), and it determines the size of mesoscale eddies. On slowly rotating exoplanets, the Rossby deformation radius determines the size of gyre circulations (Edson et al. 2011; Haqq-Misra et al. 2018). The Rossby deformation radius for the ocean is $0.42R_E$ when $P = 40$ days and decreases to $0.07R_E$ (Figure A2) when $P = 5$ days, which is consistent with the much smaller gyre circulation in the latter case (Figure 1(a)).

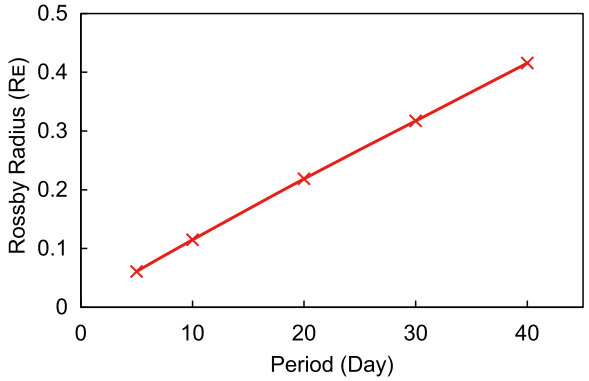

Figure A2. Planetary average Rossby deformation radius for different rotational (orbital) periods. The unit is Earth radius (R_E).

A.3. Oceanic Heat Transport from Dayside to Nightside

The dayside-to-nightside (D-to-N) oceanic heat transport (OHT) is calculated by

$$HT_{\text{ocean}} = \left| \iint_{A_{\text{ET}}} U_{\text{ET}} \cdot T_{\text{ET}} \cdot dA - \iint_{A_{\text{WT}}} U_{\text{WT}} \cdot T_{\text{WT}} \cdot dA \right| \cdot \rho \cdot C \quad \text{(A1)}$$

Where U is zonal velocity, T is ocean temperature, A is area of the vertical cross section at the eastern (90° E) and western (90° W), ρ is seawater density, and C is the heat capacity of seawater. The subscript ET implies eastern terminator, while WT implies western terminator. The unit is converted to PW, with 1 PW = 10^{15} W.

The D-to-N OHT is calculated for all 50 cases for both $P = 40$ days and 5 days. The D-to-N OHT is ∼100 PW when the continent lies on the equator, while this could increase to ∼2000 PW when the continent is located to the northeast of the substellar point (Figures 2(c) and (f)). The total D-to-N OHT is dominated by the heat transport of equatorial jet in all cases (Figure A3(d)). The GMST and global sea-ice fraction are highly correlated with the total D-to-N OHT (Figures A3(a) and (c)), indicating that changes in ocean circulation play a critical role in the climate differences between cases. The climate differences could also be caused by the different OHT from the low-latitude to the high-latitude regions by the gyre circulations. This secondary effect is not explored in the current study.

A.4. Upwelling of Ocean Water

The upwelling of ocean water is important for nutrient supply. The strength of this upwelling is represented by the vertical velocity at the base of the mixed layer as shown in Figure A4.

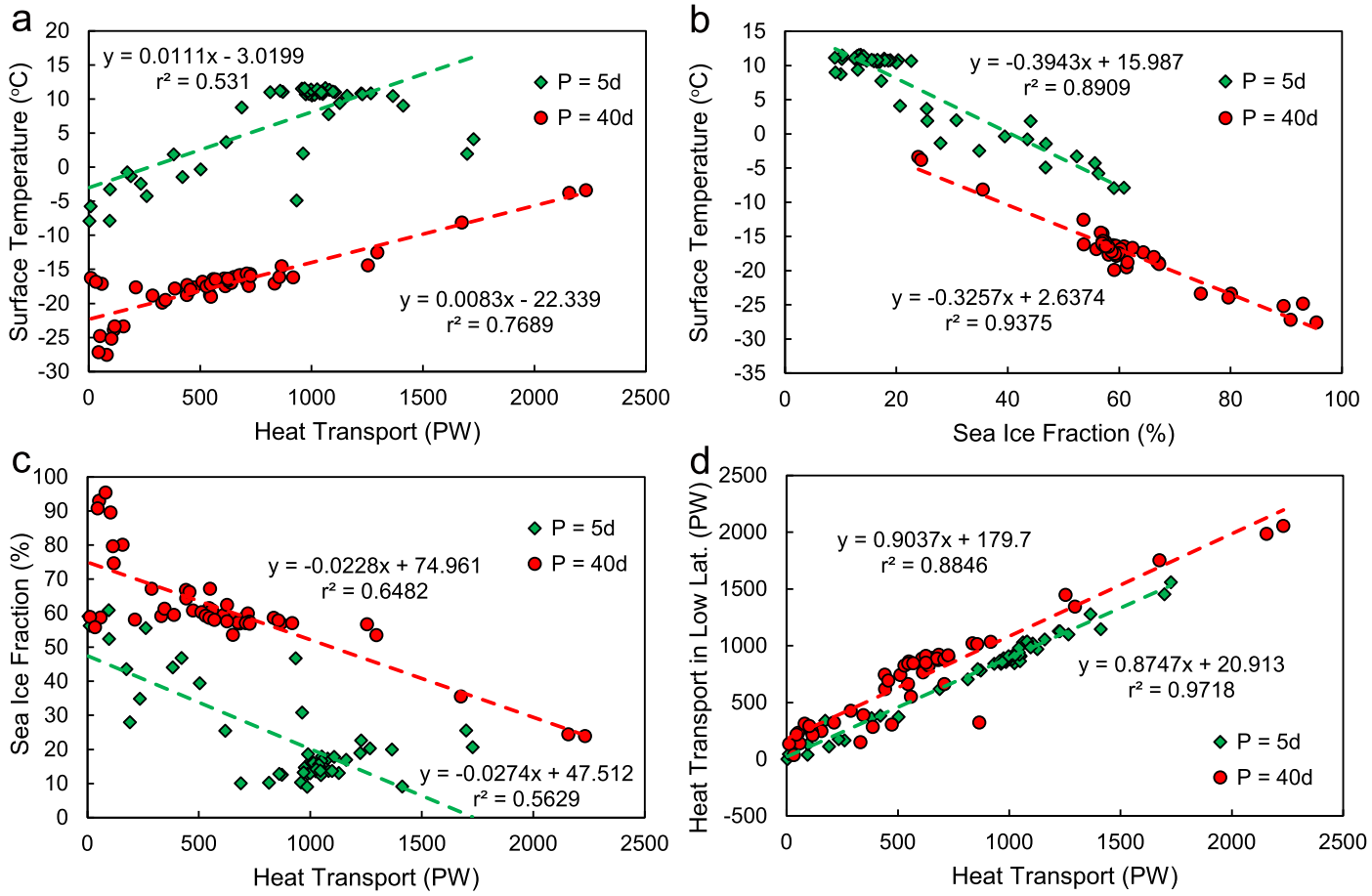

Figure A3. Relationship between (a) GMST and OHT from dayside to nightside; (b) GMST and global ice fraction; (c) global ice fractionation and OHT from dayside to nightside; (d) OHT from dayside to nightside within the low latitude (between 40° N and 40° S) and across the whole latitudinal range (90° S to 90° N). The green diamonds and red circles are for rotational periods of 5 days and 40 days, respectively.

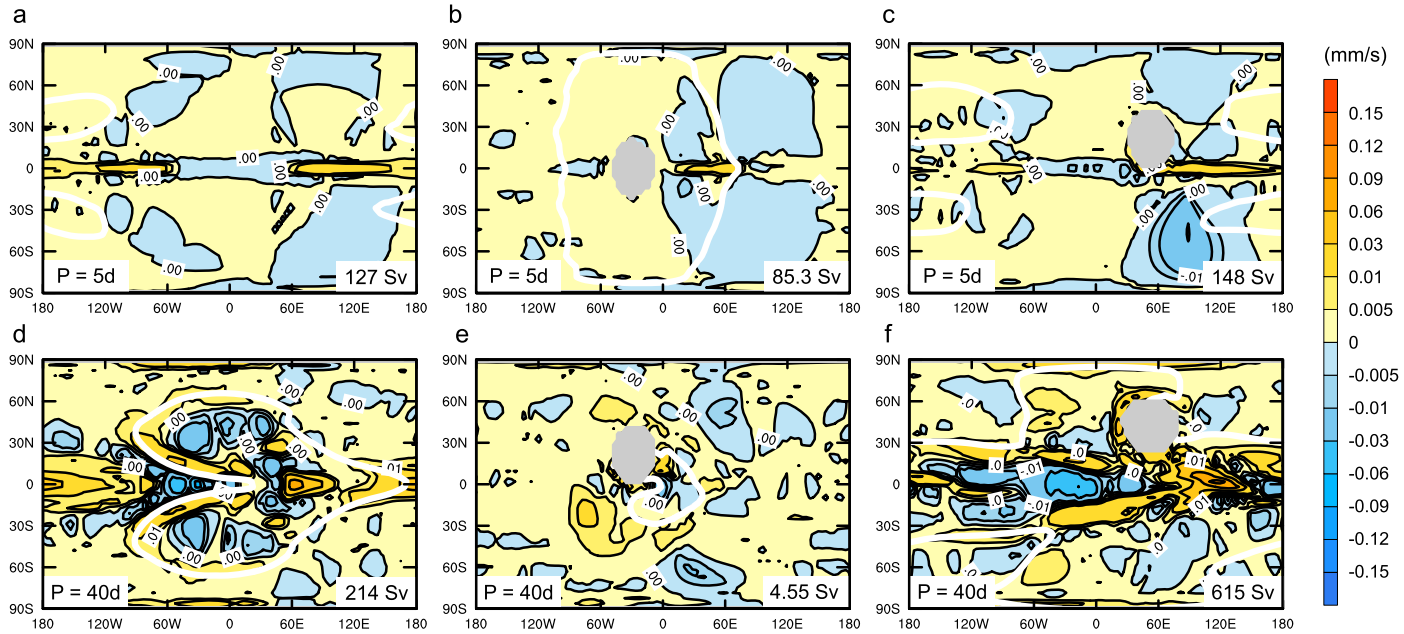

Figure A4. Vertical ocean velocity at the base of mixed layer for selective cases. The rotational period and the total upwelling at the base of mixed layer on open ocean are marked in the bottom-left and bottom-right corners, respectively. The sea ice edge on ocean surface is marked by a thick white line. The rotational and orbital period is set to 5 Earth days in (a)–(c) and 40 Earth days in (d)–(f). (a), (d) is an aquaplanet. A round land with radius of 20° is set at (0° N, 30° W) in (b), (20° N, 50° E) in (c), (20° N, 30° W) in (e), (40° N, 50° E) in (f), respectively. The positive value corresponds to the upward stream. Unit is mm s^{-1}.

References

Anglada-Escude, G., Guillem, A. P. J., Barnes, J., et al. 2016, Natur, 536, 437
Barnes, R. 2017, CeMDA, 129, 509
Chelton, D. B., deSzoeke, R. A., Schlax, M. G., Naggar, K. E., & Siwertz, N. 1998, JPO, 28, 433
Chen, H., Wolf, E. T., Kopparapu, R., Domagal-Goldman, S., & Horton, D. E. 2018, ApJ, 868, L6
Chen, H., Zhan, Z., Youngblood, A., et al. 2020, NatAs, 5, 298
Collins, W. D., Bitz, C. M., Blackmon, M. L., et al. 2006, JCLI, 19, 2122
Del Genio, A. D., Way, M. J., Amundsen, D. S., et al. 2019, AsBio, 19, 99
Dittmann, J. A., Irwin, J. M., Charbonneau, D., et al. 2017, Natur, 544, 333
Dressing, C. D., & Charbonneau, D. 2015, ApJ, 807, 45
Edson, A., Lee, S., Bannon, P., Kasting, J. F., & Pollard, D. 2011, Icar, 212, 1
Gill, A. E. 1980, QJRMS, 106, 447
Gillon, M., Triaud, A. H. M. J., Demory, B.-O., et al. 2017, Natur, 542, 456
Haqq-Misra, J., Wolf, E. T., Joshi, M., Zhang, X., & Kopparapu, R. K. 2018, ApJ, 852, 67
Hu, Y., & Yang, J. 2014, PNAS, 111, 629
Kasting, J. F., Whitmire, D. P., & Reynolds, R. T. 1993, Icar, 101, 108
Lewis, N. T., Lambert, F. H., Boutle, I. A., et al. 2018, ApJ, 854, 171
Liu, Y., Peltier, W. R., Yang, J., & Vettoretti, G. 2013, CliPa, 9, 2555
Matsuno, T. 1966, JMeSJ, 44, 25
Morley, C. V., Kreidberg, L., Rustamkulov, Z., Robinson, T., & Fortney, J. J. 2017, ApJ, 850, 121
Noda, S., Ishiwatari, M., Nakajima, K., et al. 2017, Icar, 282, 1
Olson, S. L., Jansen, M., & Abbot, D. S. 2020, ApJ, 895, 19
Peyrous, R. 1990, Ozone: Science & Engineering, 12, 19
Poulsen, C. J. 2002, GeoRL, 29, 1515
Salazar, A. M., Olson, S. L., Komacek, T. D., Stephens, H., & Abbot, D. S. 2020, ApJ, 896, L16
Shields, A. L., Bitz, C. M., Meadows, V. S., Joshi, M. M., & Robinson, T. D. 2014, ApJ, 785, L9
Showman, A. P., & Polvani, L. M. 2010, GeoRL, 37, L18811
Showman, A. P., & Polvani, L. M. 2011, ApJ, 738, 71
Turbet, M., Leconte, J., Selsis, F., et al. 2016, A&A, 596, A112
Wieczorek, M. A. 2007, in Treatise on Geophysics, vol. 10, ed. G. Schubert, 10 (Amsterdam: Elsevier), 165
Yang, J., & Abbot, D. S. 2014, ApJ, 784, 155
Yang, J., Boué, G., Fabrycky, D. C., & Abbot, D. S. 2014, ApJ, 787, L2
Yang, J., Cowan, N. B., & Abbot, D. S. 2013, ApJ, 771, L45
Yang, J., Ji, W., & Zeng, Y. 2019, NatAs, 4, 58
Yates, J. S., Palmer, P. I., Manners, J., et al. 2020, MNRAS, 492, 1691